

Interaction Studies Between Indomethacin Nanocrystals and PEO/PPO Copolymer Stabilizers

Peng Liu • Tapani Viitala • Alma Kartal-Hodczic • Huamin Liang • Timo Laaksonen • Jouni Hirvonen • Leena Peltonen

Received: 27 February 2014 / Accepted: 15 August 2014 / Published online: 22 August 2014
© Springer Science+Business Media New York 2014

ABSTRACT

Purpose The lack of effective screening methods and systemic understanding of interaction mechanisms complicates the stabilizer selection process for nanocrystallization. This study focuses on the efficiency of stabilizers with various molecular compositions and structures to stabilize drug nanocrystals.

Methods Five structurally different polymers were chosen as stabilizers for indomethacin nanocrystals. The affinity of polymers onto drug surfaces was measured using surface plasmon resonance (SPR) and contact angle techniques. Nanosuspensions were prepared using the wet-ball milling technique and their physico-chemical properties were thoroughly characterized.

Results SPR and contact angle measurements correlated very well with each other and showed that the binding efficiency decreased in the order L64 > I7R4 > F68 ≈ T908 ≈ T1107, which is attributed to the reduced PPO/PEO ratio and different polymer structures. The electrostatic interactions between the protonated amine of poloxamines and ionized indomethacin enhanced neither the affinity nor the properties of nanosuspensions, such as particle size and physical stability.

Conclusions A good stabilizer should have high binding efficiency, full coverage, and optimal hydrophobic/hydrophilic balance. A high affinity combined with short PEO chains (L64, I7R4) caused poor physical stability of nanosuspensions, whereas moderate binding efficiencies (F68, T908, T1107) with longer PEO chains produced physically stable nanosuspensions.

KEY WORDS interaction studies • nanocrystals • PEO/PPO copolymer • surface plasmon resonance (SPR) • wet-ball milling

P. Liu • T. Laaksonen • J. Hirvonen • L. Peltonen (✉)
Division of Pharmaceutical Technology, Faculty of Pharmacy, University of Helsinki, P.O. Box 56, 00014 Helsinki, Finland
e-mail: leena.peltonen@helsinki.fi

T. Viitala • A. Kartal-Hodczic • H. Liang
Division of Biopharmaceutics and Pharmacokinetics, Faculty of Pharmacy
University of Helsinki, P.O. Box 56, 00014 Helsinki, Finland

INTRODUCTION

Nanocrystallization is an efficient way to enhance the drug dissolution rate and bioavailability of poorly soluble drugs (1). Drug nanocrystals are submicron sized particles with a crystalline active pharmaceutical ingredient (API) core covered by a stabilizer layer. Besides enhanced dissolution rate the other possible main benefits of drug nanocrystals are: 1) high drug loading (i.e. mainly consisting of pure API), 2) increased adhesiveness to mucosa, 3) potential for targeted drug delivery, 4) improved bioavailability, 5) reduced fed/fasted state variability and/or 6) reduced gastric irritancy. (2–4).

In nanocrystallization, the selection of the stabilizer is a critical step. Rather a limited number of stabilizers can be used in nanosuspension production, when considering the safety of stabilizers, feasibility of stabilizers for further processing and varied requirements in different formulations and administration routes. Stabilizers frequently reported in literature are polymeric stabilizers, such as povidones (5,6), pluronics (7,8) and celluloses (9,10); and surfactant stabilizer, such as polysorbate 80 (11), sodium lauryl sulfate (12,13) and vitamin TPGS (14). There is no single versatile stabilizer suitable for all APIs; each API needs a specific stabilizer because of its distinctive physico-chemical properties. The lack of effective screening methods and systemic understanding of interactions between the drug and stabilizer makes the choice of the stabilizer difficult and time consuming.

A limited number of systematic studies related to the selection of stabilizer can be found from the literature (15). Lee *et al.* (6) studied nanomilling of 11 drug compounds with five stabilizers and two kinds of ionic surfactants. They found that the surface energy of the stabilizer and drug appeared to be an important factor for successful nanocrystallization. Eerdenbrugh *et al.* (16) screened 13 different stabilizers at three concentrations for nine structurally different drug compounds. They concluded that surfactants gave the best stabilizing performance in contrast to semi-synthetic and synthetic

linear polymers. The hydrophobicity of the drug surfaces was decisive for the agglomeration tendency of the particles. However, often too many variables with stabilizers and drug compounds make the systematic analysis complicated. Accordingly, the effect of molecular weight has been studied with different HPMC grades as a stabilizer for nabumetone nanocrystals (17), whereas Lee *et al.* (18,19) studied the interactions by using polymers with different amine acid units in order to understand the effect of chain composition, morphology and functional groups on drug nanocrystal stabilization. As of today, the selection of proper stabilizer for nanocrystallization is mostly based on trial and error.

Pluronic® and Tetronic® also known as poloxamers and poloxamines, respectively, belong to a family containing more than 50 different commercial amphiphilic block copolymers of hydrophilic poly(ethylene oxide) (PEO) and hydrophobic poly(propylene oxide) (PPO) (20). They have been widely investigated in the pharmaceutical and biomedical fields, such as thermo-sensitive hydrogels, nanoparticle/micelle carriers, and particle surface coating and tissue scaffolds (21,22). Many of them are approved by FDA as food additives and pharmaceutical ingredients (23). Pluronics® are nonionic linear triblock copolymers and consist of a hydrophobic central segment of PPO and two hydrophilic side segments of PEO (Table I), which are well known as ABA type polymers (i.e. A and B stand for PEO and PPO, respectively). Pluronic® Reverse has a reverse structure as compared to Pluronic®, i.e. a block copolymer with terminal secondary hydroxyl groups, which is also called telechelic polymer or BAB type polymer. Poloxamine encompasses a branched 4-arm (X-shape) structure and two tertiary amine groups in the center of the molecule, which renders the poloxamines positively charged and pH sensitive (23).

The aim of the present study was to gain an insight into the interaction mechanisms of stabilizers with the drug nanocrystals during wet-ball milling. Two linear poloxamers

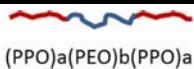
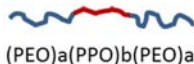
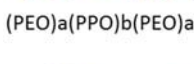
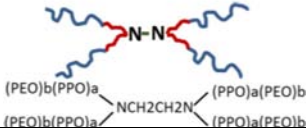
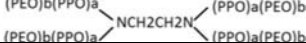
(L64 and F68), a reverse-sequential poloxamer (17R4), and two X-shaped protonated poloxamines (T908 and T1107) were chosen for the study. All the selected polymers are widely studied in drug delivery applications. Indomethacin was used as a model drug since it is poorly water-soluble and can be negatively charged in water (pH around 6) owing to a carboxyl group in the molecule. Firstly, the affinities of polymers on the indomethacin surfaces were evaluated using surface plasmon resonance (SPR) and contact angle techniques. To the best of our knowledge, this is the first time to use the SPR technique as a tool for monitoring stabilizer-drug interactions for nanocrystal research. Thereafter, the drug nanosuspensions with different stabilizers were prepared by using the wet milling technique and characterized in correlated aspects, including particle size, size distribution, zeta potential, morphology, dissolution rate, re-dispersibility and physical stability. Based on these results it was possible to present a model of the organization of polymers on the nanocrystal surface, and the interaction mechanisms between the drug and the stabilizers.

MATERIALS AND METHODS

Materials

Indomethacin (IND, Hawkins, MN, USA) was used as a model drug for wet-ball milling. Pluronic® F68 and 17R4, Tetronic® 908 and 1107 (BASF, Ludwigshafen, Germany) and Pluronic® L64 (Aldrich, Steinheim, USA) were used as stabilizers. Potassium hydrogen phthalate (Sigma, St. Louis, MO, USA), sodium hydroxide (NaOH, Sweden), ethanol (96%, *v/v*, Primalco, Rajamäki, Finland) and acetonitrile (HPLC grade, VWR International, Pennsylvania, USA) were used in dissolution tests and HPLC analyses. In all the experiments the water was ultrapurified Millipore® water (Millipore, Molsheim, France).

Table I The polymers used as stabilizers and their main properties. PEO% means the weight percent of the PEO chain. The data in the table is quoted from reference (43)

Polymer	PEO (%)	Average molecular weight (g/mol)	HLB	pKa	Physical state at 25 °C	PEO and PPO chain length and structure
17R4	40	2650	7-12	-	liquid	a=14, b=24 
L64	40	2900	15	-	liquid	a=13, b=30 
F68	80	8400	29	-	solid	a=80, b=27 
T1107	70	15000	18-23	5.6, 7.9	solid	a=20, b=60 
T908	80	25000	> 24	5.2, 7.9	solid	a=21, b=114 

Contact Angle Measurement

The contact angle between indomethacin powder compacts and aqueous stabilizer solution was measured with the sessile drop method (CAM 200, Attension/Biolin Scientific Oy, Espoo, Finland). Indomethacin bulk material (140 mg) was compressed to a disc under the compression force of 9.8 kN for 30 s by using a Specac Hydraulic Press Model 15.011 (Specac, Kent, UK) with a 13 mm diameter flat faced punch. A drop of stabilizer solution in water (0.1%, w/v) was applied to the indomethacin tablet. The contact angle was analyzed using the Attension software (Attension/Biolin Scientific Oy, Espoo, Finland). Each sample was measured in triplicate.

Surface Plasmon Resonance (SPR) Measurements

The interaction strength between the stabilizers and indomethacin was determined by surface plasmon resonance analysis (SPR). Indomethacin was deposited on the gold SPR sensor surface by keeping the sensor slide overnight in an ethanol solution containing 4 mg/ml indomethacin. The thickness of the indomethacin layer formed on the sensor surface was obtained through optical modeling of the full SPR spectrum measured in water of the indomethacin coated SPR sensor surface by using the Winspall software v. 3.02. The Winspall software was developed in Prof. Wolfgang Knoll's group at the Max-Planck-Institute for Polymer Research (Mainz, Germany) and is publicly available (24). The real-time SPR sensograms during the interaction of corresponding stabilizers and indomethacin were obtained by measuring the change in the SPR angle during the injection of a series of solutions with increasing concentrations of the corresponding stabilizer over the indomethacin coated sensor. The interaction kinetics between the stabilizers and indomethacin was analyzed by using the TraceDrawer software v. 1.4 (RidgeView Instruments Ab, Uppsala, Sweden). The topography of indomethacin coated sensor was measured with an NTEGRA Prima (NT-MDT, Russia) atomic force microscope (AFM).

Wet-Ball Milling

Nanosuspensions were prepared using the wet-ball milling technique. Bulk indomethacin (1 g) was dispersed in 5 ml aqueous stabilizer solutions with different amounts of stabilizer (0.4 g (40% relative to the drug amount) and 0.05 g (5%)). The suspensions were put in the milling vessel containing 30 g of zirconium oxide beads (\varnothing 1 mm) as milling pearls. The milling vessel and a counter weight were then placed into a planetary ball mill (Pulverisette 7 Premium, Fritsch Co., Idar-Oberstein, Germany) and grinding was performed at 1,100 rpm. One milling cycle took 3 min, and after each milling cycle there was a 15 min pause to cool down the

milling machine. Total milling time was 6 min (2 cycles), 18 min (6 cycles) or 30 min (10 milling cycles). After milling, the nanosuspensions were separated and collected from the milling pearls by a pipette. All the milling tests were repeated three times.

Freeze-Drying of Nanosuspensions

Nanosuspensions were frozen in liquid nitrogen and then dried in a freeze-dryer (Heto LyoPro 3000, Denmark). Redispersibility of dried nanosuspensions was studied by dispersing the dried powder in saturated aqueous indomethacin solution containing 0.1% (w/w) stabilizer. Saturated solutions were prepared by filtration of drug suspensions after 24 h of shaking equilibration, then through a 0.22 μ m filter membrane (Pall Co., Mexico). After vortex shaking and sonication for 3 min, the particle size and size distribution were measured by dynamic light scattering (DLS).

Particle Size and Zeta Potential

The obtained nanosuspensions were sonicated for 3 min time and diluted appropriately (ca. 30 μ g/ml) by filtration of saturated indomethacin solution containing 0.1% (w/w) of stabilizer. Mean particle size and size distribution of the nanosuspensions were determined using DLS at 25°C with a scattering angle of 90° (Malvern Zetasizer 3000HS, Malvern Instrument, Malvern, UK). For zeta potential, diluted samples of the nanosuspensions were injected to the zeta cell and measured using the same instrument. The results were recorded as the average of three measurements.

Scanning Electron Microscopy

Nanosuspension morphology was assessed by scanning electron microscopy (SEM, JSM-7,500 F, JEOL Ltd., Japan). For sample preparation, 1 drop of the nanosuspension was placed onto a carbon-coated double-sided tape, dried under ambient conditions and sputter-coated with platinum (Q150T Quommm, Turbo-Pumped Sputter Coater, China).

Stability Testing

The physical stability of the nanosuspensions was evaluated by particle size and SEM measurements during the storage period. The suspensions were diluted by 20 times, kept in a closed clear glass vessel, and stored at three different temperatures, including 4°C, room temperature and 40°C. At pre-determined storage time points, particle size analyses and SEM morphology measurements were performed.

In Vitro Dissolution Study

Dissolution profiles of nanosuspensions with 40% of stabilizer concentrations were obtained using a USP dissolution apparatus (Erweka DT-06, Heusentamm, Germany) Type II (paddle method). A known amount of sample was dispersed in 600 ml of phthalate buffer (pH 5.0) to maintain sink conditions at 37°C. The agitation speed was set to 100 rpm. At predetermined time intervals, 5 ml aliquots were withdrawn and the same amount of fresh dissolution medium was added to the vessel. Samples were filtered by Acrodisc® syringe filters with a 0.2 µm GHP membrane (PALL Life Science, Ann Arbor, MI, USA). The first 4.5 ml of the filtrate was discarded. The remaining filtrate was analyzed by high-performance liquid chromatography (HPLC). Each dissolution experiment was performed in triplicate.

The indomethacin content in milled nanosuspensions was determined by HPLC (Agilent 1100 series, Agilent technologies, Germany) with a Gemini-NX 3 µ C18 110A (100 × 4.6 mm) column (Phenomenex Co., Torrance, CA, USA). Known amounts of nanosuspensions were weighted and dissolved in ethanol. The ethanol solution was diluted with ethanol:water mixture (1:1, *v/v*) (25).

Statistical Analysis

All statistical analyses were undertaken using ANOVA test followed by Tukey's test for multiple comparisons at $p < 0.05$ with Origin software program.

RESULTS AND DISCUSSION

In order to investigate the interaction mechanisms between polymer stabilizers and API in drug nanocrystals, five polymers (17R4, L64, F68, T908 and T1107) with different PEO chain lengths and different molecular structures were chosen as stabilizers for wet milling studies. The polymers and their properties are listed in Table I.

Affinity of Polymer on Drug Surface

Contact Angle

The contact angles during the initial contacts of the stabilizer solutions with the surface of the indomethacin compressions were measured in order to illustrate the affinity between the stabilizers and the drug (Fig. 1a). As can be seen in Fig. 1a, all the curves show that the contact angles decrease fast at the beginning and then leveled out. The highest contact angle was seen with pure water, followed by the stabilizers T908, F68 and T1107. The lowest contact angles were observed with

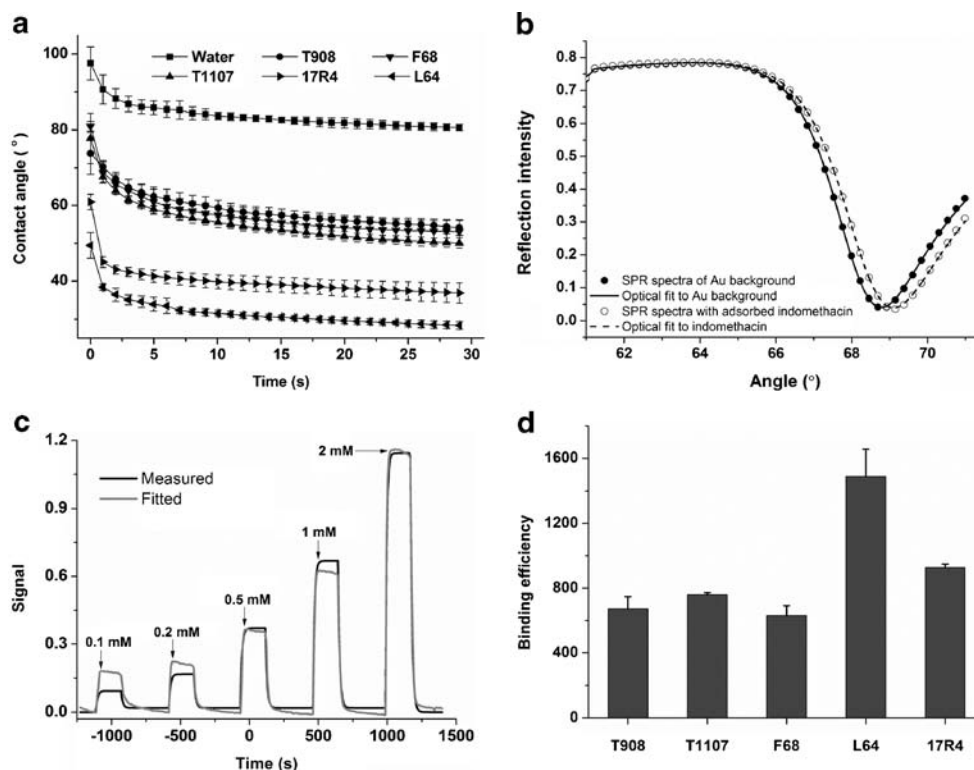
stabilizers 17R4 and L64. The water contact angle measurement is a typical method to characterize the hydrophilic/hydrophobic properties of a solid materials. The contact angle can also be used to evaluate the affinity/wettability of a drug by a stabilizer solution and to predict an appropriate stabilizer for drug milling (10,26,27). A small contact angle between the stabilizer and the drug indicates a high affinity/wettability. Based on the contact angle measurements the strength of the affinity of the stabilizers to the drug followed the order L64 > 17R4 > T1107 ≈ F68 ≈ T908. No significant differences were found between T1107, F68 and T908.

SPR Measurements

The deposition of indomethacin on the SPR sensor surface for interaction measurements with different stabilizers was achieved by precipitating indomethacin on the sensor slide from an ethanol solution. SPR spectra of the pure SPR sensor surface and the same sensor surface after depositing indomethacin on the sensor are shown in Fig. 1b. The clear shift of 0.32° in the main SPR peak position corresponds to a mass areal density of ~300 ng/cm² of indomethacin deposited on the sensor surface. Optical modeling of the SPR spectra shows that the thickness of the indomethacin layer deposited on the sensor slide was 1.5 nm when using 1.55 as the refractive index for indomethacin (28). The surface coverage and thickness of the indomethacin layer on the sensor surface is in the same range when comparing to self-assembled monolayers of thiolates on metal surfaces, which typically form 1–3 nm thick organic layers with a maximum surface coverage of 4.5×10^{14} molecules/cm² (29). The mass areal density of a typical self-assembled thiol with the same molecular weight as indomethacin would thus be ~270 ng/cm². This indicates that indomethacin forms an evenly distributed layer on top of the sensor surface enabling the use of this model surface for studying the interaction strength between different stabilizers and indomethacin. The homogeneity of the indomethacin layer on the sensor surface was also verified by atomic force microscopy (AFM) imaging (not shown). No drug crystals were visible when imaging the indomethacin layer with AFM, which is probably due to the fact that the formed indomethacin layer is very thin and that the deposition conditions used did not allow for any crystal growth to take place.

Figure 1c shows a typical example of the real-time SPR signal response as well as the kinetic fit to the measured data during the interaction of a stabilizer with indomethacin. The kinetic fit provides the maximum adsorption capacity of the stabilizer on the indomethacin surface (i.e. R_{\max}) and the equilibrium dissociation constant (i.e. K_D). The R_{\max} and K_D values were then used to determine the binding efficiency, i.e. $BE = R_{\max} / K_D$, for the interaction between the different stabilizers and indomethacin. The binding efficiency approach was originally suggested by Gustafsson *et al.* (30) for

Fig. 1 (a) Contact angle measurements of 0.1% (w/v) stabilizer solutions on compressed bulk indomethacin tablets ($n = 3$). (b) Full SPR spectra of a pure gold sensor surface (solid line) and a sensor surface with an indomethacin layer (dashed line). Dots are measured data points and lines are optical fits with the Vinspall software. (c) SPR signal response and kinetic fit to the measured data points during the interaction of the T1107 stabilizer with the indomethacin layer deposited on the SPR sensor surface. (d) Binding efficiency of different polymers for the indomethacin layer deposited on the SPR sensor surface.



determining the interaction strength between drug leads and serum proteins. This approach takes into account the difference in the molecular weight of the different stabilizers and provides the means to compare the interaction strength between the different stabilizers and indomethacin independently of the complexity of the interaction mechanism. Therefore, the higher the binding efficiency is the stronger the interaction between the stabilizer and indomethacin. The binding efficiencies for indomethacin of the five different stabilizers used in this study are shown in Fig. 1d. The binding efficiency decreases in the order $L64 > 17R4 > F68 \approx T908 \approx T1107$. Accordingly, the binding efficiency obtained from SPR measurements agreed very well with the contact angle results reflecting the affinity.

The reason for a higher binding efficiency of L64 and 17R4 compared to F68, T908 and T1107 is probably due to the differences in the structure and composition of the polymers. The L64 and 17R4 stabilizers are low molecular weight polymers with a lower hydrophilic-lipophilic balance (HLB) value compared to the high molecular weight linear F68 and branched as well as charged T908 and T1107 polymers. The total amount of PPO segments in the L64, 17R4 and F68 stabilizers are of similar length and size, and because of the hydrophobicity of the PPO segment, a thermodynamic driving force causes the polymers to adsorb on the lipophilic drug surface. The L64 and 17R4 polymers most probably adsorb onto the lipophilic indomethacin surface through their hydrophobic PPO groups by forming trains

with short PEO tails (in the case of L64) and loops (in the case of 17R4) protruding from the surface. However, the F68 polymer forms long tails with long PEO chains protruding from the surface because the relative amount of PEO (80%) is much higher compared to L64 (40%) and 17R4 (40%). This could also explain the lower binding efficiency for F68 compared to L64 and 17R4, because the long PEO tails protruding from the surface would induce steric hindrance for the polymers to adsorb very close to each other. The interaction of the branched and charged stabilizers T908 and T1107 with the indomethacin surface are probably determined by a combination of hydrophobic interactions induced by the PPO groups and electrostatic interactions induced by the positive charge on the amine groups. The lower binding efficiency of T908 and T1107 compared to L64 and 17R4 is probably a consequence of the branched structure of T908 and T1107 which causes steric hindrance for the neighboring polymers to adsorb close to each other. This is also supported by the fact that the binding efficiencies are practically the same for the F68, T908 and T1107 polymers.

Milling Results

Length of Hydrophilic Chain (L64 and F68)

Nanosuspensions with a slightly larger particle size and a wider size distribution were obtained when the L64 polymer was used (367 nm, PDI=0.30) during milling, whereas more

uniform and smaller particles were obtained with the F68 polymer (287 nm, PDI=0.24) (Table II). Both of these polymers are triblock amphiphilic linear copolymers. The L64 polymer exhibits a higher affinity to the indomethacin surface compared to the F68 polymer, but it has shorter hydrophilic PEO chains (approximately 580 g/mol vs. 3,360 g/mol for one end of the PEO segment). The short PEO chains in L64 form a thinner hydrated layer and cannot sufficiently protect the newly formed nanocrystal surfaces against aggregation. The milling process is known to be a dynamic equilibrium process between agglomeration, deagglomeration and comminution (31). The agglomeration behavior decreases the milling efficiency at the specific energy input (30).

For zeta potential, the surface charge of indomethacin nanocrystals with L64 (−28 mV) was a little bit higher compared to F68 (−24 mV). Both of the L64 and F68 stabilizers are non-ionic polymers. When polymer chains adsorb on the drug particles, the hydrophilic layer formed by the PEO segments will shield the nanocrystal surfaces and make the zeta potential less negative. Short PEO chains forming a thin layer masks the charge to a lesser extent (32). Therefore, a more negative zeta potential was obtained for the L64 stabilizer.

Linear Structure of Polymers (17R4 and L64)

The L64 stabilizer was successful in stabilizing nanosuspensions with a particle size of 367 nm after milling, while the 17R4 stabilizer showed very poor milling results, i.e. the particle size was too large and out of the DLS detection range ($>3\ \mu\text{m}$) (Table II). The particles formed with the 17R4 stabilizer could even be seen by naked eye.

Photographs of milled samples in the milling vessels were taken to clarify the different functions of the two polymers in the milling process (Fig. 2). Fig. 2a shows the indomethacin nanosuspensions with the L64 stabilizer after milling and cooling down for 1 h. A cooling period of 1 h was necessary before opening the milling vessel, because the heat and pressure generated during milling do not allow to opening the milling vessel immediately after stopping the milling process. The drug had sedimented and a liquid phase was clearly visible on top of the sediment, indicating that the sample was

not stable. After simple mixing by using a glass rod, a white homogenous nanosuspension with a low viscosity could be obtained (Fig. 2b). In the case of the 17R4 stabilizer (Fig. 2c), the milling process could be considered as a centrifugation process, because the drug and the milling pearls adhered tightly together to form a solid chunk separated from the water. After breaking the chunk and mixing it with the water by using a glass rod, a suspension with a high viscosity was obtained. Both of the re-dispersed suspensions were not stable and tended to sediment immediately.

There are two hypotheses for the milling results in presence of the 17R4 stabilizer. Firstly, the drug remained in the form of microparticles during and after milling. Secondly, the drug was actually fractured into nanocrystals, which were then aggregated into microparticles. Bilgili *et al.* (33) reported that an aggregated suspension has a higher shear viscosity than a well dispersed suspension, because aggregates can occlude liquid in their void space and increase the effective volume fraction of the solid in a suspension with fixed solid loading. Based on this explanation and the formation of a highly viscous suspension when re-dispersing the chunk formed during the milling with the 17R4 stabilizer, the second hypothesis seemed to be correct, i.e. the large particles were indeed nanoparticle aggregates. Later drug dissolution studies also confirm this conclusion. Additionally, the 17R4 polymer has a similar molecular weight and percentage of the hydrophilic moiety as L64, but in a reverse order. This telechelic polymer structure of 17R4 could promote inter-particle aggregation, which will be described in detail below.

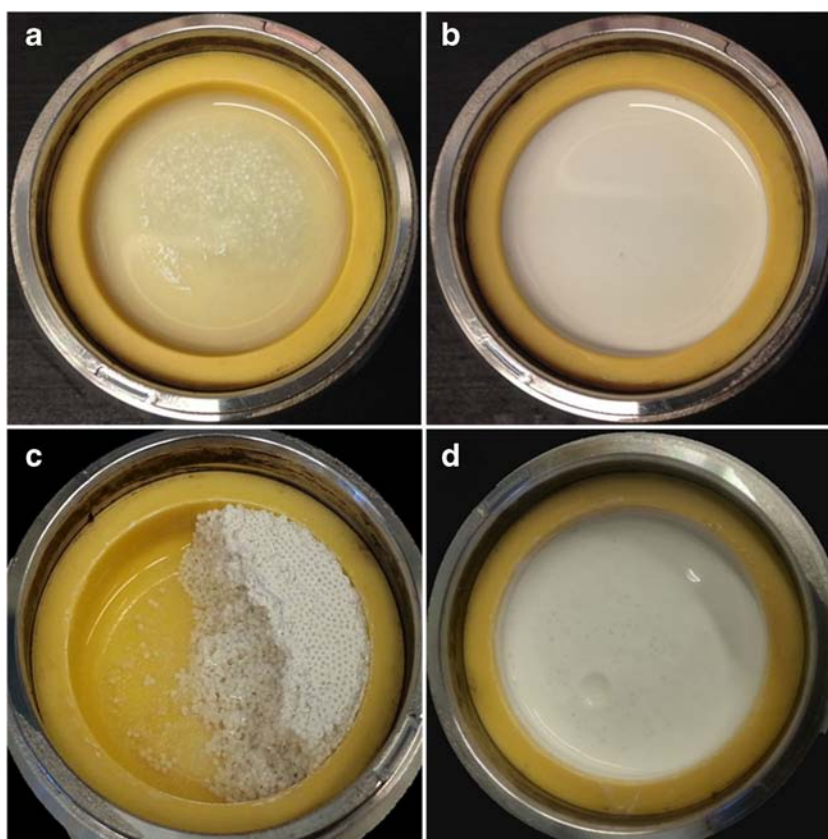
Linear and X-shape Structures (F68, T908, T1107)

The nanosuspensions were firstly prepared with 0.4 g of stabilizer. No statistically significant differences in particle size and PDI were found between the IND nanosuspensions with the F68, T908 and T1107 stabilizers (Table II). However, differences in zeta potentials were seen between the non-ionic stabilizer (F68) (−24 mV) and the protonatable stabilizers (T908 (−14 mV) and T1107 (−16 mV)). This may be attributed to two reasons. On one hand, the T908 and T1107 polymers form a denser hydrated PEO layer which shields the charged indomethacin surface more efficiently compared to the PEO layer formed with the F68 polymer. Although these three stabilizers shows a similar affinity to the indomethacin surface, the hydrophilic layers of the T908 and T1107 stabilizers encompass four PEO segments per molecule compared to two PEO segments per molecule in the case of the F68 polymer. On another hand, the T908 and T1107 polymers are also protonated in water. Protonated polymers may neutralize the negative charge of the drug particles, thus causing a lower zeta potential compared to the non-ionic F68 stabilizer.

Table II Effect of the type of stabilizer on the mean particle size, polydispersity index and Zeta potential in the presence of 0.4 g stabilizer ($n = 3 \pm \text{s.d.}$)

Stabilizer	Size (nm)	PDI	Zeta (mV)
17R4	$> 3\ \mu\text{m}$	1	–
L64	367 ± 16	0.30 ± 0.04	-28 ± 1
F68	287 ± 2	0.24 ± 0.01	-24 ± 3
T1107	307 ± 24	0.26 ± 0.02	-16 ± 0
T908	286 ± 15	0.22 ± 0.01	-14 ± 3

Fig. 2 Photographs of milled suspensions with different stabilizers. **(a)** Milled sample with the L64 stabilizer after cooling for 1 h; **(b)** Mixing by hand from **(a)** sample; **(c)** Milled sample with the I7R4 stabilizer; **(d)** mixing by hand from **(c)** sample.



Indomethacin was milled in HCl solution ($\text{pH}=1.2$) with the T908 stabilizer in order to elucidate the necessity of electrostatic interactions between poloxamine stabilizers and the drug in the reduction of nanocrystal size. The diprotonated positively charged form of the ethylene diamine groups of poloxamine dominate at pH values below $\text{pK}_{\text{a}1}$, while indomethacin nanocrystals exhibit no charges on the particle surfaces at low pH values (34). Nanosuspensions with particle size of 262 nm and $\text{PDI}=0.18$ were successfully obtained without the electrostatic interactions, i.e. at pH 1.2, and the nanosuspensions also showed long-term stability (data not shown). As this particle size is very close to the size of the particles milled in a higher pH value, these results indicate that the hydrophobic interactions, rather than electrostatic interactions, are the main driving forces for the attraction between indomethacin and the T908 stabilizer. The zeta potential of the nanocrystals prepared at pH 1.2 was not

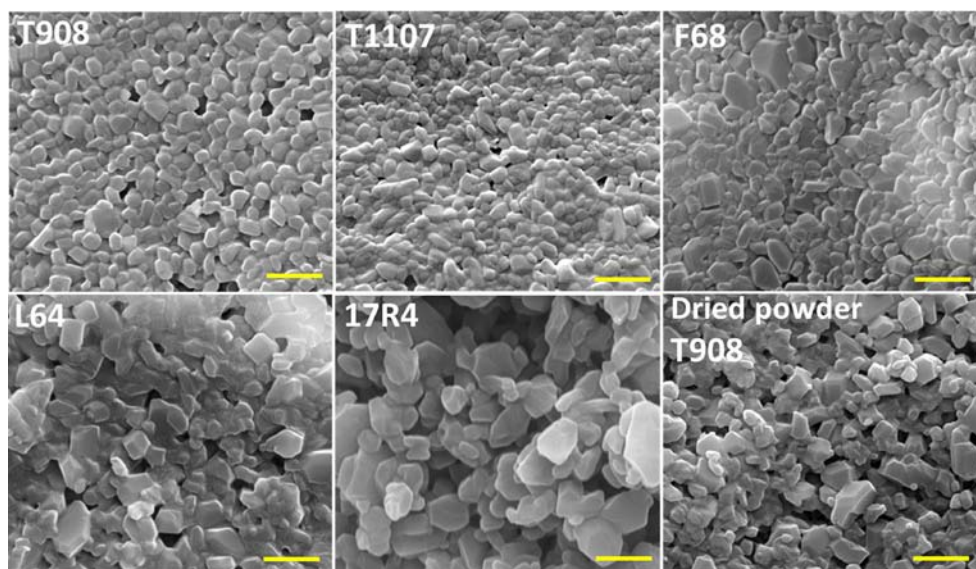
determined since the pH of the medium affects the zeta potential measurements and the zeta potential observed at pH 1.2 would not be comparable with the data in Table II.

To further understand the effect of the stabilizer structure on the particle size, the stabilizer amount was decreased to 0.05 g. Table III summarizes the particle sizes and size distributions obtained with different milling times. The IND particle size with the T908 stabilizer was decreased after two milling cycles and then increased with increasing milling time. For the other two stabilizers, the particle sizes and size distributions were decreased with the milling time. Smaller and more homogeneous nanosuspensions were obtained when F68 was used as the stabilizer. These results might be caused by the different molecular weights of the polymers. The T908 stabilizer has the largest molecular weight, followed by the T1107 and the F68. At the same stabilizer amount and milling medium volume, the order of the used stabilizer molar concentration was F68 ($1.2 \times$

Table III The particle size and size distribution of indomethacin suspensions with 0.05 g stabilizers and different milling time ($n=2$). C2, C6 and C10 in the table represents 2, 6 and 10 milling cycles of 3 min each

Stabilizer	C2		C6		C10	
	Size (nm)	PDI	Size (nm)	PDI	Size (nm)	PDI
T908	609 ± 133	0.75 ± 0.20	$1,264 \pm 791$	0.86 ± 0.20	2,590	1
T1107	$1,367 \pm 371$	1	716 ± 150	0.88 ± 0.17	580 ± 9	0.66 ± 0.09
F68	863 ± 334	0.89 ± 0.15	533 ± 34	0.57 ± 0.04	453 ± 27	0.43 ± 0.05

Fig. 3 SEM images of indomethacin nanosuspensions prepared with different stabilizers (amount of stabilizer 0.4 g): T908, T1107, F68, L64, 17R4 and dried nanopowder of indomethacin prepared with T908. All scale bars represents 1 μm .



10^{-3} mol/l) > T1107 (6.7×10^{-4} mol/l) > T908 (4.0×10^{-4} mol/l). The total surface area is increased as new fractured crystals are constantly formed during the milling. The T908 stabilizer was clearly insufficient to cover the entire particle surfaces, which caused the nanocrystals to aggregate. For the smaller molecules of T1107 and F68, the stabilizers provided the necessary steric stabilization and thus the particle size was reduced with increasing milling time.

Morphology of Indomethacin Crystals (SEM)

Figure 3 presents the SEM images of nanosuspensions prepared with the five stabilizers and one freeze dried nanopowder prepared with the T908 stabilizer. The SEM results are roughly in accordance with the DLS results. The nanosuspensions with the T908 and T1107 stabilizers showed uniform nanocrystals with a round shape, whereas several large particles with an irregular shape can be seen in the case of the F68 stabilizer. Nanocrystals were found for nanosuspensions prepared with the 17R4 stabilizer, which

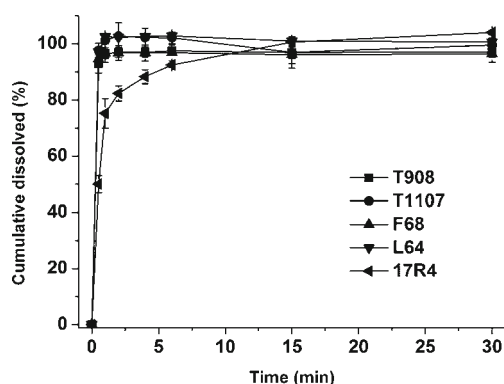


Fig. 4 Dissolution profiles of milled suspensions with the T908, T1107, F68, L64 and 17R4 stabilizers ($n=3$).

together with the results shown in Fig. 2d confirms that nanocrystals are actually formed when using the 17R4 stabilizer, but the newly formed nanocrystals agglomerate or aggregate quickly. Many larger particles can be seen for the L64 and 17R4 stabilizers, since the poor stabilizer failed to protect the nanocrystals from aggregation and therefore decreased the milling efficiency. Freeze-dried nanosuspensions with the T908 stabilizer were also imaged (Fig. 3 dried powder). The nanocrystals were intact after freeze-drying the nanosuspensions and the mean particle size was not obviously changed even without any lyoprotectant. However, the size distribution seemed to become wider in contrast to the fresh nanosuspensions. More details about the freeze-dried powders are given below.

Dissolution of Nanosuspensions

The *in vitro* dissolution profiles of milled nanosuspensions prepared with the five different kinds of stabilizers were

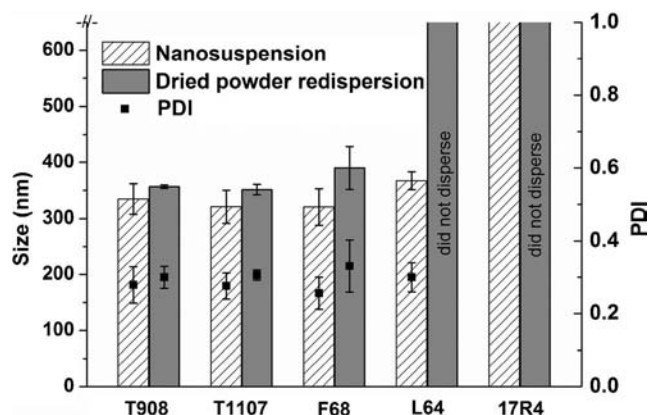
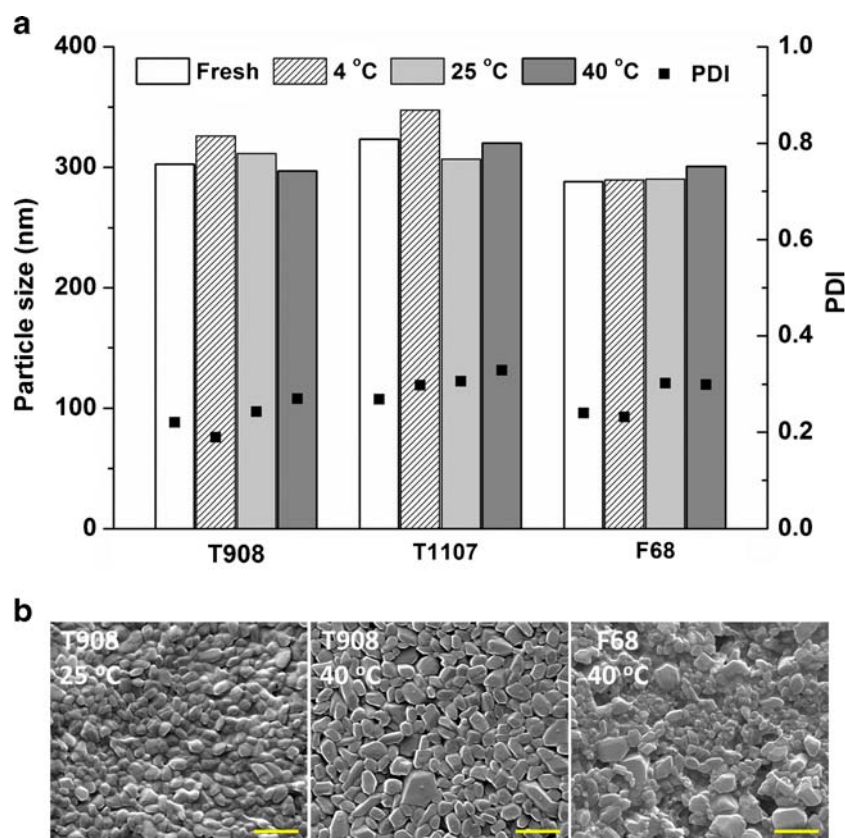


Fig. 5 The mean particle size and size distribution of original nanosuspensions and re-dispersed nanocrystal powders with 0.4 g stabilizer ($n=3$).

Fig. 6 (a) Mean particle size and size distribution of nanosuspensions as a function of temperature after storage for 1.5 years. (b) SEM images of nanosuspensions after storage for 1.5 years. The samples are: stabilizer T908 at room temperature; stabilizer T908 at 40°C; stabilizer F68 at 40°C. All scale bars represents 1 μm .



compared in sink conditions (Fig. 4). The nanosuspensions with the T908, T1107, F68 and L64 stabilizers exhibited a similar dissolution curve. Nearly 100% of the nanosized indomethacin was dissolved after 1 min, after which the dissolution curve reached a plateau. The rapid dissolution is attributed to the reduced particle size (i.e. around 300 nm), increased surface area and enhanced saturation solubility. However, suspensions with the 17R4 stabilizer showed a slower dissolution rate at the beginning. At 15 min, the dissolved amount of indomethacin reached 97%, which is close to the amount of the other four nanosuspensions, and obviously higher than the unmilled indomethacin (ca. 20%) (35). The poor steric stabilization of 17R4 leads to nanoparticle aggregation and decreased dissolution velocity in the beginning of the dissolution. However, the aggregated nanocrystals can dissociate into individual particles during the dissolution experiment and improve the dissolution rate. This finding is in accordance with the SEM results, further confirming that the microparticles formed in the presence of the 17R4 stabilizer consist of aggregated nanocrystals rather than individual larger particles.

Re-dispersibility of Freeze-Dried Nanosuspensions

The re-dispersibility of dried nanosuspensions with 0.4 g of the different stabilizers is shown in Fig. 5. For dried samples milled

with the T908, T1107 and F68 stabilizers, no statistically significant differences were observed to the fresh nanosuspensions in particle sizes and size distributions. This suggests that the dried samples retained their original particle size very well upon re-dispersion even without any protectants. Irreversible aggregation and fusion are commonly taking place during the freeze-drying process because of the entangled polymer chains on the particle surfaces, the increased contact points among nanocrystals, the disappearance of the steric repulsion of the stabilizer, and many stresses (36). Consequently, cryoprotectants, such as sugars are often used. In our case, the polymers not only act as stabilizers in the nanosuspensions, but also as protectants in the freeze-drying process. The re-dispersibility of the dried samples with the T908, T1107 and F68 stabilizers at lower stabilizer amount (0.05 g) were also tested (data not shown). These dried powders could not be re-dispersed into nanosuspensions since the low stabilizer amount failed to fully cover the particle surfaces and, thus, led to irreversible aggregation. In the cases of the L64 and 17R4 stabilizers, the dried samples could also not be re-dispersed. This might be attributed to the poor wetting ability and structure of the polymers. Moreover, both of these polymers are liquids with high viscosities at ambient temperature, which induce paste-like dried samples rather than powders. The paste-like samples are difficult to disperse in a solution.

Table IV Physical stability of nanosuspensions with the L64 stabilizer at different temperatures ($n=2$). N means not possible to determine, since the particle size was out of the detection range

Time (day)	4°C		25°C		40°C	
	Size (nm)	PDI	Size (nm)	PDI	Size (nm)	PDI
0	386	0.35	386	0.35	386	0.35
3	391	0.52	N	N	371	0.34
6	394	0.37	N	N	415	0.39
9	400	0.38	N	N	415	0.41
30	N	N	N	N	430	0.44

Stability of Nanosuspensions

Figure 6a depicts the physical stability of the nanosuspensions with the T908, T1107 and F68 stabilizers under three different temperatures after storage for 1.5 years. In contrast to the fresh nanosuspensions, the mean particle sizes of these three nanosuspensions varied within 30 nm, implying that these three polymers provided a sufficiently good stabilization for the indomethacin nanocrystals. These changes in particle sizes were independent of the temperature, which differed from the results reported by other studies. Normally, a higher temperature enhances the aggregation tendency of hydrophobic particles since the hydrophobic interaction is an endothermic entropy-driven process (37). Nonetheless, the particle size distribution (PDI) displayed an increasing trend with the elevated temperature for the three cases shown in Fig. 6. This is attributed to the Ostwald ripening, because an elevated temperature can increase the solubility of the drug (37). Fig. 6b shows the morphology of the nanosuspensions after storage for 1.5 years. Nanocrystals with a wide size distribution can be found for a higher storage temperature storage because of the Ostwald ripening, which is in accordance with the results in Fig. 6a.

In contrast to the three polymers mentioned above, the L64 polymer displayed a poor and temperature dependent stabilization capability (Table IV). At room temperature,

nanoparticles grew to microparticles after 3 days. At 4°C, the PDI of nanosuspensions increased from 0.35 to 0.52 after 3 days. After storage for 1 month, the particles settled and the sediment could not be re-dispersed or broken by sonication. Against our expectations, the nanosuspensions showed higher stability at 40°C. However, the particle size and size distribution at 40°C still increased slowly with time.

Interaction Mechanisms

Polymer-particle interactions are very complex due to a delicate balance of various enthalpic and entropic contributions (38). The adsorption behavior of organic polymers from solution to solid surfaces, such as titanium dioxide particles, latex and gold nanoparticles, has been widely investigated. It has been proposed that linear flexible homopolymers adsorb on the solid surfaces in train-loop-tail conformations (39,40), and the tails determine the hydrodynamic thickness (41). Conversely, amphiphilic block copolymers have the desired segment for anchoring to the solid surface and allow the remainder of the chain to stretch into the outer environment in either loop or tail form. The use of amphiphilic block copolymers often supplies a higher surface density and larger layer thickness on the surfaces compared to homopolymers (42). Taken this as a basis together with our experimental results, the interaction mechanisms between various PEO/PPO polymers and indomethacin nanocrystals were drawn out (Fig. 7).

The L64 polymer shows the strongest binding strength to the drug surface (Fig. 1) due to its high PPO/PEO ratio (42). Polymer L64 can stabilize the fractured nanocrystals during milling, and thus nanosuspensions could be prepared successfully. Nevertheless, these nanosuspensions were unstable during the storage (Table IV) because of the insufficient steric barrier induced by the short hydrophilic PEO chains (Fig. 7) and, consequently, the nanocrystals were aggregated. The 17R4 polymer showed the second strongest affinity to the solid drug surface, but the unfavorable molecular structures, including the short PEO chain and telechelic structure, lead to nanocrystal clusters. This aggregation behavior decreased the

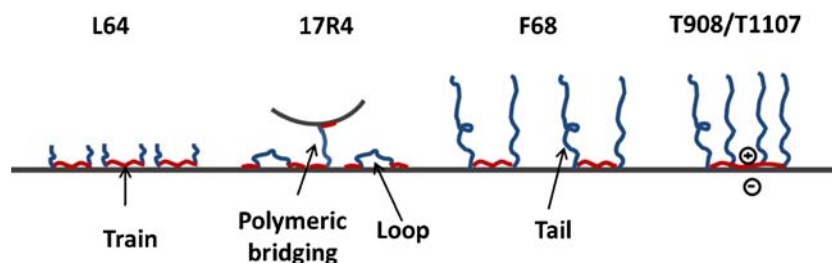


Fig. 7 A schematic diagram of interaction mechanisms between nanocrystal surfaces and stabilizers. The L64 polymer forms a long train - short tail conformation on the drug surface, which fails to protect the nanocrystals from aggregation; The 17R4 polymer with a telechelic structure forms a loop on the solid surface. The short PEO length and micellar bridging cause a serious agglomeration during the milling; The F68 polymer folds in half to anchor onto the drug surface through the PPO group, while the long PEO tails make a thick steric layer which stabilizes the nanosuspensions; The Tetronic T908 and T1107 polymers anchor onto the nanocrystal surfaces not only by hydrophobic interactions but also by electrostatic attractions. Four equal-sized PEO chains per molecule stay around the nanocrystals and stabilize the nanosuspensions.

milling efficiency (Fig. 3) and dissolution rate (Fig. 4). As illustrated in other publications, telechelic polymers such as 17R4 form loops around the hydrophobic core (Fig. 7). The flower-like micelles promote inter-particle connections via micellar bridging, where the end chains of one micelle penetrate into the cores of another micelle. The micellar bridging decreases the distance of two particles and compromise the steric repulsion and, thus, enhance the aggregation and increase the viscosity.

The binding strengths of the F68, T908 and T1107 polymers are equally lower than for the L64 and 17R4 polymers. The crowding effects produced by the long PEO blocks decrease the adsorption level of the copolymers onto the particles (42). The protonated X-shaped Tetronic polymers interact with indomethacin nanocrystals not only by electrostatic but also by hydrophobic attractions, and four equal-sized PEO subunits per molecule stay in the liquid phase to provide steric stabilization (Fig. 7). However, the special structure of Tetronic polymers seem to neither enhance the affinity nor prompt the nanosuspension properties compared to the non-ionic F68 polymer, since the particle size, re-dispersibility and stabilization capability of these three polymers were very similar.

CONCLUSIONS

The present study investigated the effect of stabilizers, including the various molecular compositions and architectures, on the properties of milled nanosuspensions as well as the binding strength of the polymer stabilizers on the indomethacin surface. We conclude that a good stabilizer in the nanocrystal system must fulfill three fundamental requirements at the same time. Firstly, the adsorbent should firmly attach to the solid surface. Secondly, the polymer should cover the particles. Thirdly, the hydrophilic/lipophilic balance of the stabilizer structure, i.e. in our case the balance between PPO and PEO chain lengths, is important to anchor the block copolymers onto the nanocrystal surfaces. The driving force for adsorption originates from the hydrophobic nature of the PPO segment. The PEO segments on one hand offer the steric hindrance to protect the nanocrystals from aggregating, but on the other hand also prevent the unabsorbed polymer from further adsorbing onto the solid surface, which decreases the binding efficacy. A high affinity and short PEO chains, as in the case of the L64 and 17R4 stabilizers, causes a poor physical stability of the nanosuspensions and poor re-dispersibility of the freeze-dried samples. With the same ratio of PPO/PEO segments, the telechelic structure of 17R4 promotes nanocrystal aggregation because of micellar bridging, as well as decrease the milling efficacy and dissolution rate. The protonated X-shaped Tetronic polymers and the non-

ionic linear polymer F68 with similar ratio of PPO/PEO segments and a train-tail conformation on the particle surface upon adsorption do not induce any differences in the affinity, particle size, dissolution rate, re-dispersibility and physical stability.

ACKNOWLEDGMENTS

The authors acknowledge The Finnish Funding Agency for Innovation (TEKES, Finland; NanoForm project 40187/11) China Scholarship Council and The Academy of Finland for financial support. M.Sc. May Mah from University of Otago and M.Sc. Dongfei Liu from University of Helsinki are acknowledged for valuable discussion and suggestions, and Dr. Petri Ihalainen for providing the AFM image of the indomethacin layer precipitated on the SPR sensor slide.

REFERENCES

1. Rabinow BE. Nanosuspensions in drug delivery. *Nat Rev Drug Discov.* 2004;3:785–96.
2. Müller RH, Gohla S, Keck CM. State of the art of nanocrystals - special features, production, nanotoxicology aspects and intracellular delivery. *Eur J Pharm Biopharm.* 2011;78(1):1–9.
3. Moschwitz JP. Drug nanocrystals in the commercial pharmaceutical development process. *Int J Pharm.* 2013;453(1):142–56.
4. Shegokar R, Müller RH. Nanocrystals: industrially feasible multi-functional formulation technology for poorly soluble actives. *Int J Pharm.* 2010;399(1–2):129–39.
5. Lindfors L, Forssen S, Westergren J, Olsson U. Nucleation and crystal growth in supersaturated solutions of a model drug. *J Colloid Interf Sci.* 2008;325(2):404–13.
6. Lee J, Choi JY, Park CH. Characteristics of polymers enabling nanocomminution of water-insoluble drugs. *Int J Pharm.* 2008;355(1–2):328–36.
7. Lai F, Sinico C, Ennas G, Marongiu F, Marongiu G, Fadda AM. Diclofenac nanosuspensions: influence of preparation procedure and crystal form on drug dissolution behaviour. *Int J Pharm.* 2009;373(1–2):124–32.
8. Xiong R, Lu W, Li J, Wang P, Xu R, Chen T. Preparation and characterization of intravenously injectable nimodipine nanosuspension. *Int J Pharm.* 2008;350(1–2):338–43.
9. Douroumis D, Fahr A. Stable carbamazepine colloidal systems using the cosolvent technique. *Eur J Pharm Sci.* 2007;30(5):367–74.
10. Cerdeira AM, Mazzotti M, Gander B. Miconazole nanosuspensions: influence of formulation variables on particle size reduction and physical stability. *Int J Pharm.* 2010;396(1–2):210–8.
11. Dolenc A, Kristl J, Baumgartner S, Planinsek O. Advantages of celecoxib nanosuspension formulation and transformation into tablets. *Int J Pharm.* 2009;376:204–12.
12. Mauludin R, Müller RH, Keck CM. Development of an oral rutin nanocrystal formulation. *Int J Pharm.* 2009;370:202–9.
13. Mauludin R, Müller RH, Keck CM. Kinetic solubility and dissolution velocity of rutin nanocrystals. *Eur J Pharm Sci.* 2009;36:502–10.
14. Guo Y, Luo J, Tan S, Otieno BO, Zhang Z. The applications of vitamin E TPGS in drug delivery. *Eur J Pharm Sci.* 2013;49:175–86.
15. Peltonen L, Hirvonen J. Pharmaceutical nanocrystals by nanomilling: critical process parameters, particle fracturing and stabilization methods. *J Pharm Pharmacol.* 2010;62:1569–79.

16. Van Eerdenbrugh B, Vermant J, Martens JA, Froyen L, Van Humbeeck J, Augustijns P, *et al.* A screening study of surface stabilization during the production of drug nanocrystals. *J Pharm Sci.* 2009;98(6):2091–103.
17. Sepassi S, Goodwin DJ, Drake AF, Holland S, Leonard G, Martini L, *et al.* Effect of polymer molecular weight on the production of drug nanoparticles. *J Pharm Sci.* 2007;96(10):2655–66.
18. Lee J, Lee SJ, Choi JY, Yoo JY, Ahn CH. Amphiphilic amino acid copolymers as stabilizers for the preparation of nanocrystal dispersion. *Eur J Pharm Sci.* 2005;24(5):441–9.
19. Lee MK, Kim S, Ahn CH, Lee J. Hydrophilic and hydrophobic amino acid copolymers for nano-comminution of poorly soluble drugs. *Int J Pharm.* 2010;384:173–80.
20. Moghimi SM, Hunter AC. Poloxamers and poloxamines in nanoparticle engineering and experimental medicine. *Trends Biotechnol.* 2000;18(10):412–20.
21. Alvarez-Lorenzo C, Sosnik A, Concheiro A. PEO-PPO block copolymers for passive micellar targeting and overcoming multidrug resistance in cancer therapy. *Curr Drug Targets.* 2011;12(8):1112–30.
22. Alvarez-Lorenzo C, Rey-Rico A, Sosnik A, Taboada P, Concheiro A. Poloxamine-based nanomaterials for drug delivery. *Front biosci (Elite ed).* 2010;2:424–40.
23. Chiappetta DA, Sosnik A. Poly(ethylene oxide)-poly(propylene oxide) block copolymer micelles as drug delivery agents: Improved hydrosolubility, stability and bioavailability of drugs. *Eur J Pharm Biopharm.* 2007;66(3):303–17.
24. Knoll W. <http://www2.mpip-mainz.mpg.de/groups/knoll/software>.
25. Liu P, De Wulf O, Laru J, Heikkilä T, Van Veen B, Kiesvaara J, *et al.* Dissolution studies of poorly soluble drug nanosuspensions in non-sink conditions. *AAPS PharmSciTech.* 2013;14:748–56.
26. Pardeike J, Müller RH. Nanosuspensions: a promising formulation for the new phospholipase A(2) inhibitor PX-18. *Int J Pharm.* 2010;391:322–9.
27. Pardeike J, Strohmeier DM, Schröedl N, Voura C, Gruber M, Khinast JC, *et al.* Nanosuspensions as advanced printing ink for accurate dosing of poorly soluble drugs in personalized medicines. *Int J Pharm.* 2011;420(1):93–100.
28. Watanabe A. A trial production of a table of the optical crystallographic characteristics of crystalline drugs including crystal habits (study of crystalline drugs by means of a polarizing microscope. *XIX Yakugaku zasshi.* 2002;122(8):595–606.
29. Love JC, Estroff LA, Kriebel JK, Nuzzo RG, Whitesides GM. Self-assembled monolayers of thiolates on metals as a form of nanotechnology. *Chem Rev.* 2005;105(4):1103–69.
30. Gustafsson SS, Vrang L, Terelius Y, Danielson UH. Quantification of interactions between drug leads and serum proteins by use of “binding efficiency”. *Anal Biochem.* 2011;409(2):163–75.
31. Mende S, Stenger F, Peukert W, Schwedes J. Mechanical production and stabilization of submicron particles in stirred media mills. *Powder Technol.* 2003;132:64–73.
32. Sezgin Z, Yüksel N, Baykara T. Preparation and characterization of polymeric micelles for solubilization of poorly soluble anticancer drugs. *Eur J Pharm Biopharm.* 2006;64(3):261–8.
33. Bilgili E, Afolabi A. A combined microhydrodynamics-polymer adsorption analysis for elucidation of the roles of stabilizers in wet stirred media milling. *Int J Pharm.* 2012;439:193–206.
34. Alvarez-Lorenzo C, Gonzalez-Lopez J, Fernandez-Tarrio M, Sanchez-Macho I, Concheiro A. Tetronic micellization, gelation and drug solubilization: Influence of pH and ionic strength. *Eur J Pharm Biopharm.* 2007;66(2):244–52.
35. Liu P, Rong X, Laru J, Van Veen B, Kiesvaara J, Hirvonen J, *et al.* Nanosuspensions of poorly soluble drugs: preparation and development by wet milling. *Int J Pharm.* 2011;411:215–22.
36. Chaubal MV, Popescu C. Conversion of nanosuspensions into dry powders by spray drying: a case study. *Pharm Res.* 2008;25(10):2302–8.
37. Verma S, Kumar S, Gokhale R, Burgess DJ. Physical stability of nanosuspensions: investigation of the role of stabilizers on Ostwald ripening. *Int J Pharm.* 2011;406:145–52.
38. Sarkar B, Venugopal V, Tsianou M, Alexandridis P. Adsorption of pluronic block copolymers on silica nanoparticles. *Colloid Surf A.* 2013;422:155–64.
39. Bergaya F, Lagaly G. *Developments in Clay Science.* Oxford: Elsevier; 2012.
40. Goodwin DJ, Sepassi S, King SM, Holland SJ, Martini LG, Lawrence MJ. Characterization of polymer adsorption onto drug nanoparticles using depletion measurements and small-angle neutron scattering. *Mol Pharm.* 2013;10:4146–58.
41. Malmsten M, Linse P, Cosgrove T. Adsorption of PEO-PPO-PEO block copolymers at silica. *Macromolecules.* 1992;25:2474–81.
42. Lambert O, Jada A, Dumas P. Adsorption of triarm starblock copolymers based on polystyrene, poly(ethylene oxide) and poly(ϵ -caprolactone) at the solid-solution interface. *Colloid Surf A.* 1998;136:263–72.
43. Jain TK, Erokku B, Dimitrijevic S, Flask CA, Labhasetwar V. Magnetic resonance imaging of multifunctional pluronic stabilized iron-oxide nanoparticles in tumor-bearing mice. *Biomaterials.* 2009;30(35):6748–56.